

# Probing the Structural Basis and Adsorption Mechanism of an Enzyme on Nano-sized Protein Carriers

Yanxiong Pan<sup>+,1</sup>, Sunanda Neupane<sup>+,1</sup>, Jasmin Farmakes<sup>1</sup>, Michael Bridges<sup>2</sup>, James Froberg<sup>3</sup>, Jiajia Rao<sup>4</sup>, Steven Qian<sup>4</sup>, Guodong Liu<sup>1</sup>, Yongki Choi<sup>3</sup>, and Zhongyu Yang<sup>\*,1</sup>

<sup>+</sup>These authors contribute equally.

1. Department of Chemistry and Biochemistry, North Dakota State University, Fargo, ND, 58108
2. Jules Stein Eye Institute, University of California, Los Angeles, Los Angeles, CA, 90025
3. Department of Physics, North Dakota State University, Fargo, ND, 58108
4. Department of Plant Sciences, North Dakota State University, Fargo, ND, 58108
5. Department of Pharmaceutical Sciences, North Dakota State University, Fargo, ND, 58108

\*Corresponding author: [zhongyu.yang@ndsu.edu](mailto:zhongyu.yang@ndsu.edu)

## 1. Protein expression, purification, and spin labeling.

Mutants of 44C, 65C, 72C, 89C, 115C, 118C, 131C, and 151C were prepared as described before.<sup>1</sup> Briefly, the DNAs of these mutants were generated by QuikChange site-directed mutagenesis of the pET11a-T4L genetic construct containing the pseudo-wild-type mutations C54T and C97A,<sup>2,3</sup> followed with verification of each mutation by DNA sequencing.<sup>4</sup> These mutants of T4L were expressed, purified, and then desalted (to remove DTT) into a buffer suitable for spin labeling (the “spin buffer”, containing 50 mM MOPS and 25 mM NaCl at pH 6.8) using previously reported procedure.<sup>2</sup> The desalted protein mutants were then reacted with a 10 fold molar excess of S-(2,2,5,5-tetramethyl-2,5-dihydro -1H-pyrrol-3-yl) methyl methanesulfothioate (MTSL, Toronto Research Chemicals, Inc., Toronto) at 4°C overnight (yielding R1). Excess MTSL was removed using the Amicon spin concentrator (Millipore, 10,000 MWCO, 50 ml). The spin-labeled protein mutants were stored in the spin buffer at -20 °C for further use.

## 2. Continuous-Wave EPR spectroscopy.

To confirm the conformational dynamics of the spin-labeled T4L, the stored samples were concentrated to ~100  $\mu$ M using the Amicon spin concentrator (Millipore, 10,000 MWCO, 50 ml). This stock was diluted by half with a 60% w/w sucrose solution to yield a concentration of ~50  $\mu$ M in 30% w/w sucrose solution. Approximately 20  $\mu$ L of sample was loaded into a borosilicate capillary tube (0.70 mm i.d./1.25 mm o.d.; VitroGlass, Inc.), which was mounted in a Varian E-109 spectrometer equipped with a cavity resonator. All continuous wave (CW) EPR spectra were obtained with an observe power of 200  $\mu$ W. All spectra were obtained with a modulation frequency of 100 kHz and a modulation amplitude of 1.0 G. The resultant data shown in Figure S1 are consistent with the data acquired on the same mutants reported in the literature.



**Figure S1.** The CW-EPR spectra of three representative spin-labeled protein in buffer with 30% sucrose. These data are consistent with the literature.<sup>2,5,6</sup> The arrows labeled with “i” and “m” indicate the spectrum of 44R1 contains an immobile and a mobile component, respectively, also consistent with the literature.<sup>5</sup> The scan range is 100 G for each spectrum.

To determine the CW-EPR spectra of spin-labeled protein after interacting with the SiNPs, each mutant were mixed with 20  $\mu$ L 5X OH-SiNPs to obtain the mixture with the protein-to-OH-SiNP ratios of 250:1 and 10,000:1. The Mixtures

for COOH-SiNPs studies have the protein-to-COOH-SiNP ratios of 250:1 and 15,000:1. Note that to form the “saturated” mixture, the samples with high molar ratios were washed extensively (at least two rounds) with water before subjected to CW EPR studies. The CNBr-activated sepharose beads samples were prepared according to a recent procedure.<sup>7</sup>

### **3. Preparation of the hydroxylated silica nanoparticles (OH-SiNPs)**

The classical Stöber method was employed to prepare the monodisperse OH-SiNPs.<sup>8</sup> Particularly, ~7.5 mL ammonia hydroxide (48 mmol) was mixed with 130 mL anhydrous ethanol in a 250 mL three-necked flask. The mixture was stirred vigorously at 50°C for ~1 hr. Then 3.75 mL TEOS (16 mmol, tetraethyl orthosilicate, reagent grade, Sigma) was mixed with 30 mL anhydrous ethanol and dropped into pre-heated (ammonia-ethanol) mixture with a stirring speed of 1500 rpm. After reaction of ~24 hrs, the suspension solution was washed with anhydrous ethanol for at least three times via centrifugation at 13,000 rpm for 30 min to remove unreacted reagent. The obtained OH-SiNPs were then redistributed in 35 mL anhydrous ethanol and stored at 4°C for further use. The original OH-SiNPs particle size was ~ 30 nm as judged by TEM (see main text).

### **4. Preparation of the amino-coated silica nanoparticles (NH<sub>2</sub>-SiNPs)**

Approximately 17.5 mL (~0.51 mmol) OH-SiNPs suspension and 100 μL ammonia hydroxide were charged into a dried 100 mL two-necked flask with magnetic stirring, followed by addition of 1.88 mL 3-(Trimethoxysilyl) propylamine (10.7 mmol, Sigma, 97%) into the suspension and reaction for 24 hrs at 60°C. The suspension was washed with anhydrous ethanol for at least three times to remove unreacted reagents and then redistributed in 17.5 mL anhydrous ethanol for further use.

### **5. Preparation of the carboxyl-coated silica nanoparticles (COOH-SiNPs)**

Before modification, ~8.8 mL (~ 0.25 mmol) suspension of NH<sub>2</sub>-SiNPs was washed with anhydrous DMF for three times via centrifugation at 13,000 rpm for 15 mins to eliminate ethanol. The final volume of the NH<sub>2</sub>-SiNPs in DMF was 10 mL. Next, 1 g succinic hydride (9.9 mmol) and 0.5 mL Triethylamine were charged into the NH<sub>2</sub>-SiNPs suspension and stirred at room temperature for 24 hrs. The suspension was washed with anhydrous ethanol for at least three times and store within ethanol at 4°C for further use.

### **6. SiNP characterization: Fourier Transformation Infrared (FTIR)**

To confirm the presence of the three SiNPs, FTIR spectra of the OH-SiNPs, the NH<sub>2</sub>-SiNPs, and the COOH-SiNPs were acquired with an FTIR spectrometer (Thermo Scientific Nicolet 8700) on potassium bromide (KBr) disk. As shown in Figure S2A, for the OH-SiNPs, the broad absorption peak at 3300-3600 cm<sup>-1</sup> and the peak at 2980 cm<sup>-1</sup> are attributed to the O–H stretching vibration on the SiNPs surface and C–H stretching vibrations of the alkyl groups, respectively. The absorption peaks at 1095, 952 and 801 cm<sup>-1</sup> were attributed to the asymmetric vibration of Si–O, the asymmetric vibration of Si–OH, and the symmetric vibration of Si–O, respectively. On NH<sub>2</sub>-SiNPs, the appearance of a new peak at

1486  $\text{cm}^{-1}$ , which is attributed to the deformation of  $-\text{NH}_2$ , indicates the existence of  $-\text{NH}_2$  group on the surface of  $\text{NH}_2\text{-SiNPs}$ . The  $\text{COOH-SiNPs}$  were confirmed by the appearance of new peaks at 1557 and 1722  $\text{cm}^{-1}$ , which are attributed to the amide and carboxyl stretching vibration, respectively.

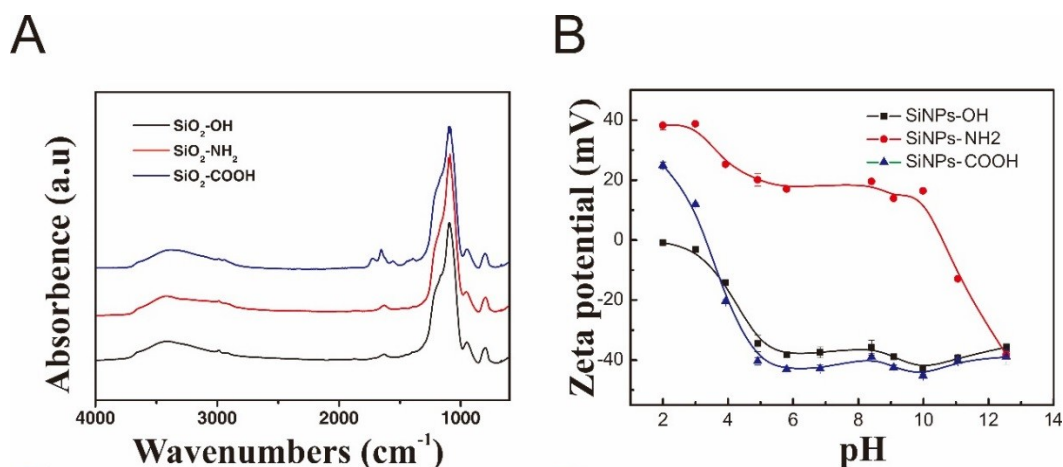


**Figure S2.** (A) The FTIR spectra of the OH-SiNPs, the  $\text{NH}_2\text{-SiNPs}$ , and the  $\text{COOH-SiNPs}$  (color-coding see inset); (B) Zeta potential changes of the  $\text{NH}_2\text{-SiNPs}$ , and the  $\text{COOH-SiNPs}$  as a function of pH (color-coding see inset).

## 7. Zeta potential measurements

To further confirm the SiNP surface modification, we conducted the Zeta potential measurements over a wide range of pH. The measurements were carried out with a Nano ZS Zetasizer (Malvern Instrument Ltd.). Typically, 5  $\mu\text{L}$  5 X SiNPs ( $\sim 0.029 \mu\text{M}$ , suspended in DD  $\text{H}_2\text{O}$ ) was mixed with 1000  $\mu\text{L}$  solution at the desired pH value, one at a time, and then subjected to measurement. The pH of each medium solution was adjusted from 2.0 to 12.55 with 0.01M HCL and 0.01 M NaOH wherein the ionic strength was fixed at 0.01 M (final NaCl concentration).

**OH-SiNPs:** Since the isoelectric point of the OH-SiNPs is close to a pH of 2.0, we observed a potential of zero at pH 2.0. As the pH was increased, the Zeta potential was decreased until reaching a plateau ( $\sim -38 \text{ mV}$ ) when  $\text{pH} > 5.8$  (Figure S2B black squares). This confirmed that at pH 7.0 the surface charge of the OH-SiNPs was negative.

**$\text{NH}_2\text{-SiNPs}$ :** The  $\text{NH}_2\text{-SiNPs}$  displayed a positive potential in a wide range of pH ( $\sim 2$  to  $\sim 10.5$ , Figure S2B red dots), confirming that the surface charge of the  $\text{NH}_2\text{-SiNPs}$  at pH 7.0 was positive. This also confirmed our rationalization of the negligible adsorption of T4L onto  $\text{NH}_2\text{-SiNPs}$  at pH 7.0 (see main text). It has to be noted that we observed strong aggregation and therefore low dispensability of  $\text{NH}_2\text{-SiNPs}$  at most pHs.

**$\text{COOH-SiNPs}$ :** The  $\text{COOH-SiNPs}$  with an isoelectric point at  $\text{pH}=2.7$  showed a similar trend as the OH-SiNPs (Figure S2B triangles). This again confirmed that at pH 7.0 the surface charge of the  $\text{COOH-SiNPs}$  was negative.

Taken together, the findings in zeta potential further confirmed the successful surface-modification of the three SiNPs.

## 8. T4L adsorption profile on SiNPs

The OH-SiNPs, the NH<sub>2</sub>-SiNPs, and the COOH-SiNPs were washed with water via centrifuging at 13000 rpm for 5 min (at least three times) to replace the ethanol with the water. These samples were then re-suspended to 5 fold (5X SiNPs). To determine adsorption profile, a representative protein mutant, 44R1, was added to 50  $\mu$ L 5X OH-SiNPs with various protein-to-SiNP ratios. The amount of adsorbed protein was computed by subtraction of the amount of protein in the supernatant of each mixture from the total protein added (the initial protein/OH-SiNP; c.f. Figure S3). The protein concentrations in stock and in the supernatant of each mixture were determined by measuring the protein optical density (OD) 280.

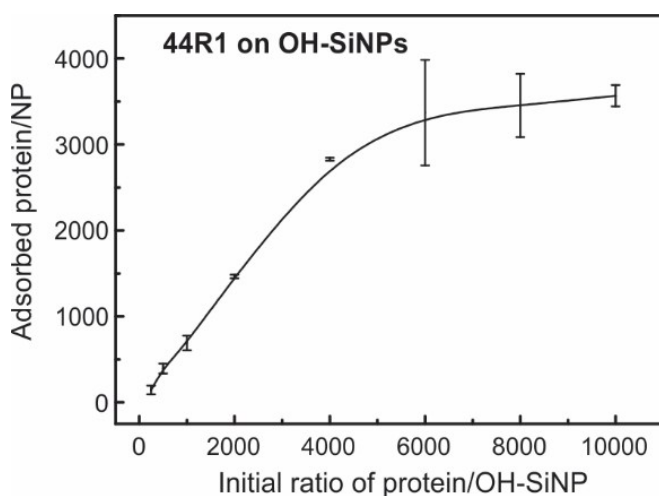


**Figure S3.** The adsorption profile of 44R1 on the OH-SiNPs. Approximately 3,500-4,000 proteins were found to be able to adsorb onto each OH-SiNP. Note there was no wash done on each protein/SiNP mixture with the protein-to-SiNP ratios indicated by the x-axis.

To perform the EPR area analysis, the OH- or COOH-SiNPs with a concentration of  $\sim 0.05 \mu$ M was mixed with the T4L enzyme and incubated at room temperature under gentle nutation. The EPR spectrum did not change after the mixture was incubated for  $>30$  min. We therefore performed all of our binding experiments following such timeline. When washing the samples, after centrifugation and removal of the supernatant, we added  $\sim 0.5$  mL water and varied the incubation time under gentle nutation at room temperature. The EPR spectra did not change after the mixture was incubated for  $> 5$  min. We therefore performed all of our unbinding experiments following such time line. Taken together, all of our EPR measurements were performed on samples under equilibrium state, and the spectral area analysis could be considered as a close approach to estimate the amount of unbound protein.

## 9. Activity

The activity assay was tested using the kit purchased from Sigma-Aldrich (*Micrococcus lysodeikticus* cells, ATCC No. 4698, M3770) as described earlier.<sup>9,10</sup> Briefly, 10 mg of the cell was suspended in 100 mL 66 mM potassium

phosphate Buffer (pH = 6.2) to obtain *Micrococcus* suspension (0.01% “substrate”). The active protein degrades the amount of the cell membrane, which was reflected by the reduction of the OD at 450 nm. Such reduction in OD was employed to monitor the amount of active protein. To prepare samples for the activity assay, the OH- and the COOH-SiNPs were mixed with a representative mutant, 44R1, at a protein-to-SiNP ratio of 250:1. The second set of samples were prepared by saturating each of the OH- and the COOH-SiNPs with 44R1. These enzyme adsorbed SiNPs were then mixed with 66 mM potassium phosphate buffer (pH = 6.24, at 25°C) to prepare 100  $\mu$ L (1  $\mu$ M) protein solution, one at a time. Lastly, 40  $\mu$ L of the SiNP/protein mixture was added into  $\sim$ 1 mL (960  $\mu$ L, precisely) of the *Micrococcus* suspension prepared as described above. The final volume of SiNPs added to the substrate was  $\sim$ 1.4  $\mu$ L. The OD at 450 nm was monitored immediately using Nanodrop after the mixture formation for 300 s.

To eliminate the possibility of SiNPs affecting OD at 450 nm, we conducted a series of control experiments. As is evident from Figure S4, the presence of the OH- and the COOH-SiNPs under our experimental conditions for the activity assay did not cause major changes in OD at 450 nm. The SiNPs only affect the OD at 450 nm at a much higher concentration (blue triangles of Figure S4).

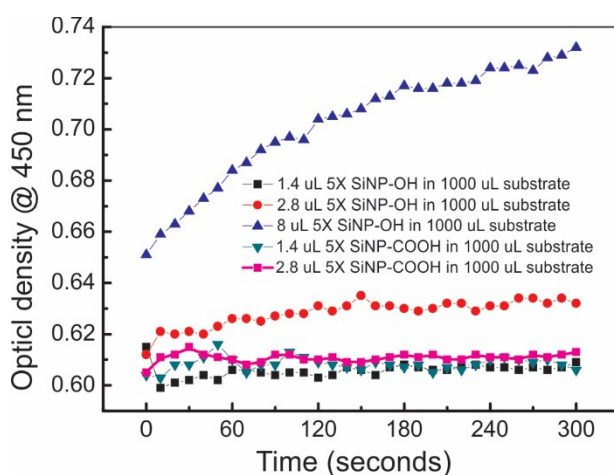


**Figure S4.** The control experiments for the activity assay. The value of 1.4  $\mu$ L was selected because that volume of SiNPs was identical to the SiNPs we used for the protein activity test.

## 10. DEER EPR

Four-pulse DEER data at 80K were obtained on an ELEXSYS 580 spectrometer operated at Q-band. The protein concentration was at or below 200  $\mu$ M. Samples of  $\sim$ 20  $\mu$ L in water in a glass capillary (1.4 i.d.  $\times$  1.7 o.d.; VitroCom, Inc.) were flash frozen in liquid nitrogen. A 36-ns  $\pi$ -pump pulse was set at the maximum absorption spectra, and the observer  $\pi/2$  (16 ns) and  $\pi$  (32 ns) pulses were positioned 50 MHz (17.8 G) upfield, which corresponds to the absorption maxima of the center-field line.

The time domain signal are shown in Figure S5, wherein the black curves are the

raw data after baseline correction, and the red curves are the fit generated with the “LongDistances”. This program is written in LabVIEW (National Instruments) and can be downloaded from [www.chemistry.ucla.edu/directory/hubbell-wayne-l](http://www.chemistry.ucla.edu/directory/hubbell-wayne-l). Several baseline correction approaches were investigated, and the resultant distance distributions were found to be not sensitive to the baseline function. The presented signal are obtained with a variable dimension baseline equipped with the software.

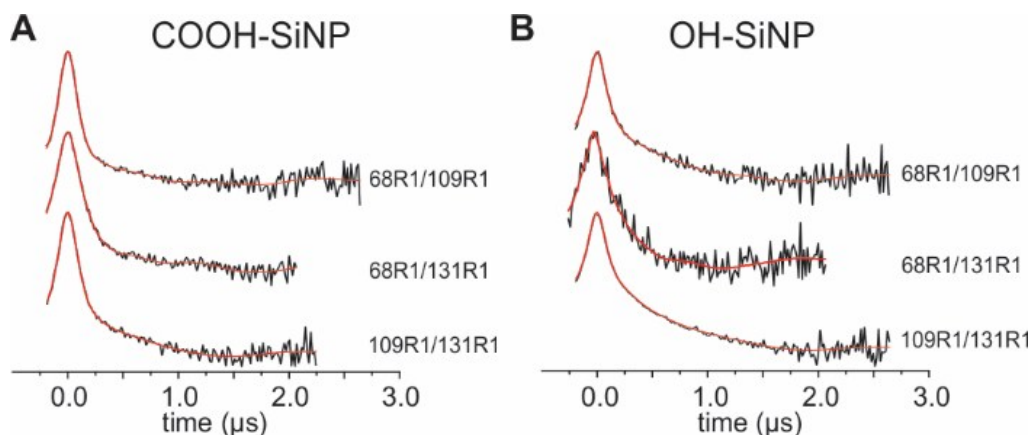


**Figure S5.** The baseline corrected DEER signal (black) for three spin labeled pairs of T4L adsorbed onto the OH-SiNPs (A) and the COOH-SiNPs (B). The fit obtained using “LongDistances” are shown in red.

## 11. CD spectroscopy

To further probe the secondary structural changes of enzyme adsorption and to confirm the conformational perturbation indicated by DEER EPR, we conducted the Circular Dichroism spectroscopy for the protein attached to the OH- and the COOH-SiNPs. A doubly labeled mutant of T4L used for the DEER studies, the 109R1/131R1, was used in CD. Our positive control was the same sample dissolved in water.

The CD spectra were obtained (Jasco J-815- 15OS, Japan) from 260 to 200 nm using a cylindrical cuvette with 1 mm path length. Typical sample volume and concentration were 300 μL and 10 mM, respectively. The baseline of each sample was corrected using DD-water.

As shown in Figure S6, the data of the enzymes adsorbed to the SiNPs are relatively noisier, even though the final protein concentration for all of the three involved samples was adjusted to be identical (50 μM). We rationalized the higher noise level to the scattering effects of particles. Nevertheless, a significant reduction in the peak of 208 nm, which is the characteristic peak for helical structures, for protein adsorbed to the OH- and the COOH-SiNPs indicate a significant secondary structural change in the protein upon adsorption. This conclusion is consistent with findings from DEER.



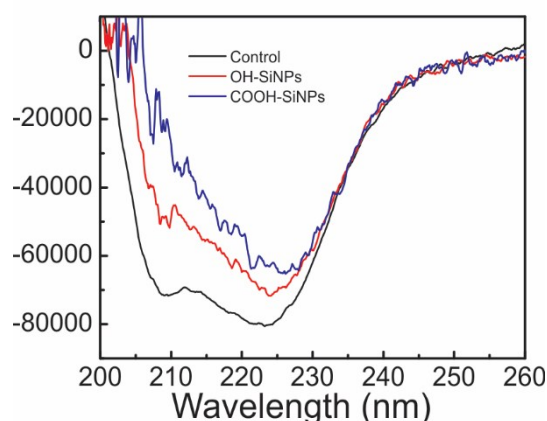


**Figure S6.** The CD spectra of T4L mutant 109R1/131R1 in water (black) and adsorbed to the OH- (red) and the COOH- (blue) SiNPs.

## 12. Desorption

Desorption experiments were conducted for both saturated OH- and COOH-SiNPs. In detail, a representative mutant, 151R1, was adsorbed to both SiNPs and washed with  $2 \times 200 \mu\text{L}$  HCl buffer (pH = 3.0, ionic strength  $\sim 0.01$  M in NaCl) via centrifugation at 13,000 rpm for 5 min. The supernatants after each wash were combined and concentrated using the Amicon Ultra-0.5 mL Centrifugal Filters (10 K cut-off). The CW EPR spectra of the mutants in water, on each SiNP, and those of SiNPs after wash are presented in Figure S6.

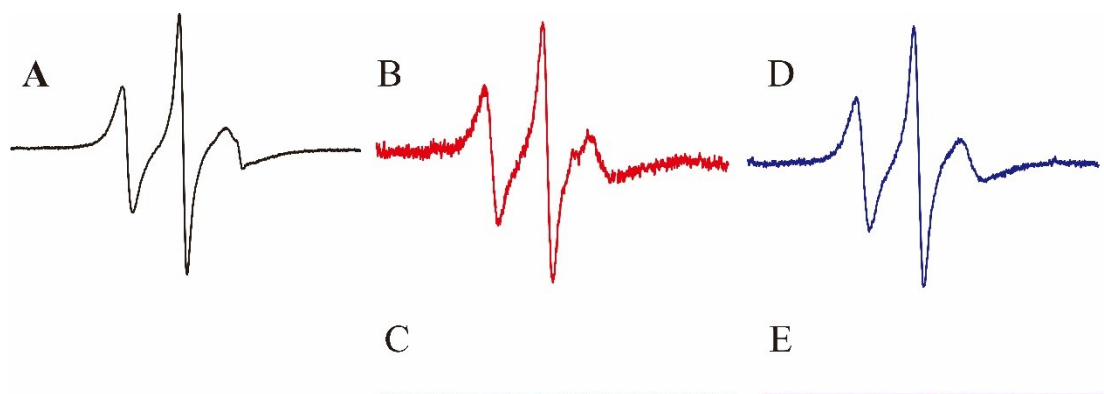


**Figure S7.** The EPR spectra of T4L mutant 151R1 in water (A), supernatants after T4L desorption from the OH-SiNPs (B) and the COOH-SiNPs (D), and those of the OH-SiNPs (C) and the COOH-SiNPs (E) after desorption.

## 13. Influence of ionic strength.

The 300 mM is about twice ionic strength of the physiological saline, which is about the ionic strength that we anticipate to break down the charge-charge interaction in our system. The influence of ionic strength on enzyme adsorption



was conducted as follows.

*First*, we confirmed via CW EPR that, for the site of 44R1, the conformational dynamics in water with no salt remains unchanged as compared to that in 100 and 300 mM NaCl (Figure S8A and reference 54). This is reasonable given the stability of the protein.

*Next*, prior to loading enzymes under different ionic strength, ~20  $\mu$ L of each SiNP was washed with ~500  $\mu$ L of the corresponding solution for at least three times, in order to ensure complete medium-switch. The protein was also switched to the corresponding medium before loading. Then, the protein-to-SiNP ratios of 10,000:1 and 15,000:1 was loaded for the OH- and the COOH-SiNPs, respectively, for each ionic strength. After incubation for at least 30 mins, the CW EPR spectrum for each sample were acquired (Figure S8). For the COOH-SiNPs, at higher salt concentrations (100 and 300 mM), there was almost no adsorption since there was no additional broadening observed (Figures S8A *VS* S8B). Washing with the corresponding solution resulted in almost no EPR signal, indicating complete desorption (Figure S8C). At 25 mM NaCl, the additional broadening (arrow of Figure S8B) is noticeable, indicating adsorption occurs. Washing with the same solution resulted in a small amount of broadened EPR signal (arrow of Figure S8C), indicating that at this low salt concentration, the adsorption of enzyme to the COOH-SiNP surface is effective, although the loading capacity is low.

*Lastly*, for the OH-SiNPs, even at 100 mM salt concentration, noticeable broadening (arrows of Figure S8D) can be observed, and washing did not completely diminish the adsorption. As the salt concentration was decreased to 25 mM, the amount of enzyme adsorption was increased.

Taken together, our ionic strength studies indicate that at the COOH- surface, ionic strength has a bigger impact on the adsorption than in the case of OH-surface.

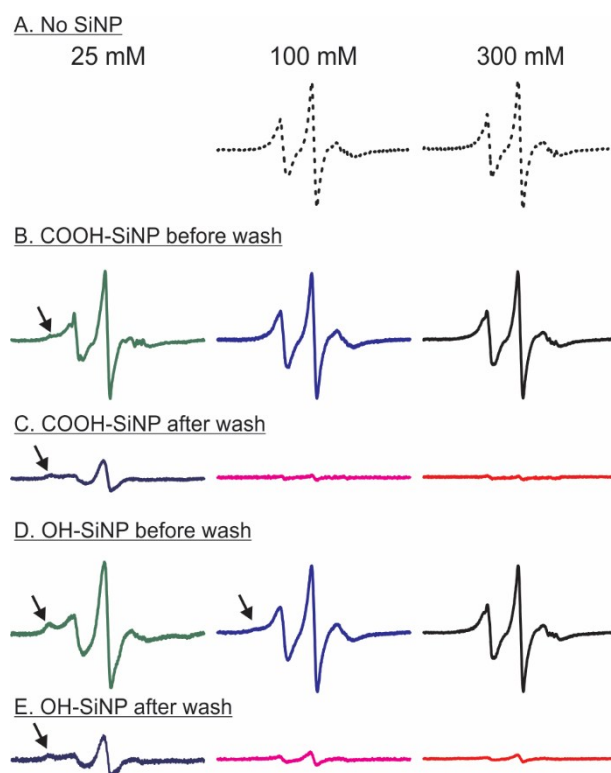


**Figure S8.** The EPR spectra of 44R1 in different NaCl concentrations (A), 44R1 upon adsorption to the COOH-SiNPs (B) and the OH-SiNPs (D) at different NaCl concentrations. After washing with the corresponding solutions, the EPR signal of the COOH-SiNPs (C) and the OH-SiNPs (E) at different NaCl concentrations were also acquired.

#### 14. Atomic Force Microscopy Imaging

The four nanoparticle solutions (1. COOH-SiNPs, 2. OH-SiNPs, 3. T4L-COOH-SiNPs, 4. T4L-OH-SiNPs) were prepared in a water solution ( $\sim 5 \mu\text{M}$ ). The samples were prepared by incubating  $10\text{-}\mu\text{L}$  of each solution on silicon substrates (University Wafer) for 10 min in a sealed compartment to protect evaporation at room temperature. The samples were then washed with de-ionized water (Millipore), and dried under purified air flow. The Imaging measurements were performed using a commercial atomic force microscope (NT-MDT NTEGRA AFM). The samples were imaged under ambient conditions in semi-contact mode with a resonant frequency of 190 kHz AFM probes (Budget sensors).

#### 15. Dynamic light scattering.

The hydrodynamic diameter of SiNPs in the absence and presence of T4L were determined via dynamic light scattering by using the Zetasizer (NICOMP 380 ZLS Particle Sizer, Particle Sizing Systems, Inc. USA). For each measurement,  $2 \mu\text{L}$  solution ( $\sim 0.05 \mu\text{M}$ ), either with or without T4L, was mixed with 1 mL distilled-deionized (DD) water and transferred into a disposable flint glass tube with plain end. The intensity of the incident laser light was tuned closed to 250 KHz in order to measure the particle size. Details of operation followed the standard user's guide provided by the manufactory.

In general the hydrodynamic radii determined by DLS are larger than the radii determined by TEM. DLS offers an opportunity to probe the polydispersity of the COOH- and the OH-SiNPs. Specifically, for the COOH-SiNPs, DLS indicated a dominant diameter at 154 nm (70%) and a minor diameter at 572 nm (30%), the latter of which was possibly originated from minor/local aggregation of the particles. For the OH-SiNPs, the dominant diameter was 123 nm (74%) while the minor diameter was 480 nm (26%). Upon saturation with T4L enzyme, the COOH-SiNPs showed a dominant diameter at 903 nm (90%) and a minor diameter at 282 nm (10%). Such enhancement in size is consistent to the multiple-layer protein adsorption. The OH-SiNPs show a dominant diameter at 711 nm (88%) and a minor diameter at 103 nm (12%). The smaller hydrodynamic radius of the OH-SiNPs is consistent with the findings that a COOH-SiNPs is able to adsorb more proteins than an OH-SiNP.

#### References:

1. Yang, Z.; Jiménez-Osés, G.; López, C. J.; Bridges, M. D.; Houk, K. N.; Hubbell, W. L. *J. Am. Chem. Soc.* **2014**, *136*, 15356-15365.
2. López, C. J.; Fleissner, M. R.; Guo, Z.; Kusnetzow, A. K.; Hubbell, W. L. *Protein Sci.* **2009**, *18*, 1637-1652.
3. Fleissner, M. R.; Brustad, E. M.; Kálai, T.; Altenbach, C.; Cascio, D.; Peters, F. B.; Hideg, K.; Peuker, S.; Schultz, P. G.; Hubbell, W. L. *Proc. Natl. Acad. Sci.* **2009**, *106*, 21637-21642.
4. Matsumura, M.; Wozniak, J. A.; Sun, D. P.; Matthews, B. W. *J. Biol. Chem.* **1989**, *264*, 16059-16066.
5. Guo, Z.; Cascio, D.; Hideg, K.; Hubbell, W. L. *Protein Sci.* **2008**, *17*, 228-239.
6. Langen, R.; Oh, K. J.; Cascio, D.; Hubbell, W. L. *Biochemistry* **2000**, *39*, 8396-8405.
7. López, C. J.; Fleissner, M. R.; Brooks, E. K.; Hubbell, W. L. *Biochemistry* **2014**, *53*, 7067-7075.
8. Stöber, W.; Fink, A.; Bohn, E. *J. Colloid Interface Sci.* **1968**, *26*, 62-69.
9. Bower, C.; Xu, Q.; McGuire, J. *Biotech. Bioengin.* **1998**, *58*, 658-662.
10. Bower, C.; Sananikone, S.; Bothwell, M.; McGuire, J. *Biotech. Bioengin.* **1999**, *64*, 373-376.